



Published in final edited form as:

*Chem Phys Lett.* 2008 July 20; 460(1-3): 187–190. doi:10.1016/j.cplett.2008.05.082.

## Gold Nanoparticle Based Surface Enhanced Fluorescence For Detection of Organophosphorus Agents

Samuel S. R. Dasary, Uma S. Rai, Hongtao Yu, Yerramilli Anjaneyulu, Madan Dubey<sup>1</sup>, and Paresh Chandra Ray

Department of Chemistry, Jackson State University, Jackson, MS 39217, USA

<sup>1</sup>US Army Research Laboratory, 2800 Powder Mill Road Adelphi, MD 20783

### Abstract

Organophosphorus agents (OPA) represent a serious concern to public safety as nerve agents and pesticides. Here we report the development of gold nanoparticle based surface enhanced fluorescence (NSEF) spectroscopy for rapid and sensitive screening of organophosphorus agents. Fluorescent from  $\text{Eu}^{3+}$  ions that are bound within the electromagnetic field of gold nanoparticles exhibit a strong enhancement. In the presence of OPA,  $\text{Eu}^{3+}$  ions are released from the gold nanoparticle surface and thus a very distinct fluorescence signal change was observed. We discussed the mechanism of fluorescence enhancement and the role of OPA for fluorescence intensity change in the presence of gold nanoparticles.

### Introduction

Organophosphorus (OP) nerve agents are organic esters of phosphorous-based acid derivatives that have uses in chemical warfare, terrorism, and pesticides<sup>1–10</sup>. Detection and neutralization of major OPs to protect human life is a major challenge around the world. The challenge has generated tremendous demands for innovative tools capable of detecting major OPs in a simpler and reliable manner in real time on demand at the desired places. Sarin, soman, *O*-ethyl-*S*-(2-diisopropylaminoethyl) methylphosphonothioate (VX) and *O*-isobutyl-*S*-2-diethylaminoethyl methylphosphonothioate (R-VX), belonging to the organophosphorus (OP) group, are highly toxic nerve agents. Rapid identification of the appropriate nerve agents will allow first responders and emergency personnel to make the important decisions concerning barricading, evacuating, or efficient decontamination of a particular site and will prevent them from becoming victims themselves. The sensor needs to be inexpensive, portable, reliable, absent of false positives and available to all military and first responders. Current analytical techniques<sup>1–10</sup> such as gas and liquid chromatography, are very sensitive and reliable, but cannot be carried out in the field, are time-consuming and expensive, and have to be performed by highly trained technicians. Biological methods<sup>1–10</sup>, such as immunoassays and inhibition of acetylcholinesterase activity, for OP determination have also been reported. Despite the promise of immunoassay techniques, since these methods require long analysis time (1–2 h) and extensive sample handling (several washing steps), they are unsuitable for online monitoring of detoxification processes. The nanoscience revolution that sprouted throughout the 1990s is having a great impact on current and future sensor technology around the world<sup>11–33</sup>. Their extremely small size enables them to access a variety of biological environments; their size also endows them with valuable size dependent properties that can be exploited in applications. The benefits of nanotechnology make it ideal for sensor development, for environmental and biological

monitoring<sup>11–33</sup>. Finally, their large surface areas are platforms for engineering multifunctional systems. Recently surface enhanced spectroscopy shows great promises for detection of DNA/RNA, cancer cell and bio-agents<sup>15,16,18,20–26,29</sup>. Driven by the need, in this letter we report the development of ultra-sensitive gold nanoparticle based surface enhanced fluorescence (NSEF) spectroscopy<sup>20–26</sup> for screening organophosphorus agent (OPA). We have used three organophosphorus agents as shown in Scheme 1.

## 2. Experimental Methods

Hydrogen tetrachloroaurate ( $\text{HAuCl}_4 \cdot 3\text{H}_2\text{O}$ ),  $\text{NaBH}_4$ ,  $\text{NaCl}$ , sodium citrate, europium (III) nitrate hydrate, pinacolyl methylphosphonate, methylphosphonic acid, glyphosate were purchased from Sigma-Aldrich and used without further purification.

Gold nanoparticles (15 nm or larger) were synthesized using reported method<sup>12–14, 17–19, 27–29</sup>. In brief, 0.01% solution (100 mL) of  $\text{HAuCl}_4 \cdot 3\text{H}_2\text{O}$  was brought to boiling under stirring and 3 mL of 1% (wt) solution of sodium citrate was added to the boiling solution. The solution underwent a series of color changes until it turned wine red and the boiling was continued for further 30 min. After cooling to room temperature, the gold nanoparticle solution was diluted to 100 mL using deionized water. Gold nanoparticles of different sizes and shapes were synthesized by controlling the ratio of  $\text{HAuCl}_4 \cdot 3\text{H}_2\text{O}$  and sodium citrate as reported recently<sup>11–33</sup>. Transmission electron microscope (TEM) and UV-visible absorption (as shown in Figure 1) spectra were used to characterize the nanoparticles. The particle concentration was measured by UV-visible spectroscopy using the molar extinction coefficients at the wavelength of the maximum absorption of each gold colloid as reported recently [ (15)  $518\text{nm} = 3.6 \times 10^8 \text{ cm}^{-1} \text{ M}^{-1}$ , (30)  $530\text{nm} = 3.0 \times 10^9 \text{ cm}^{-1} \text{ M}^{-1}$ , (40)  $533\text{nm} = 6.7 \times 10^9 \text{ cm}^{-1} \text{ M}^{-1}$ , (50)  $535\text{nm} = 1.5 \times 10^{10} \text{ cm}^{-1} \text{ M}^{-1}$ , (60)  $540\text{nm} = 2.9 \times 10^{10} \text{ cm}^{-1} \text{ M}^{-1}$ , and (80)  $550\text{nm} = 6.9 \times 10^{10} \text{ cm}^{-1} \text{ M}^{-1}$  ]<sup>12–14,17–19,27–29</sup>. Europium nitrate  $\text{Eu}(\text{NO}_3)_3$  was dissolved in  $\text{H}_2\text{O}$  to make 1 mM transparent and colorless solution. Gold colloid in solution was added to the  $\text{Eu}(\text{NO}_3)_3$  solution (1:1) with gentle mixing and allowed to stay for 2 hrs. Fluorescence measurements were performed using FluoroMax-2 spectrofluorometer.

## Results and Discussion

The use of lanthanide ions as spectroscopic probes of structure and content is an established technique<sup>34–35</sup>. The narrow excitation and emission peaks of lanthanide spectra provide highly sensitive and selective analyses. The fluorescence spectrum of europium (III) solution excited at 395 nm has five emission peaks at 458 nm, 535 nm, 555 nm, 590 nm and 615 nm, resulting from  $^5\text{D}_3 \rightarrow ^7\text{F}_4$ ,  $^5\text{D}_1 \rightarrow ^7\text{F}_1$ ,  $^5\text{D}_1 \rightarrow ^7\text{F}_2$ ,  $^5\text{D}_0 \rightarrow ^7\text{F}_1$  and  $^5\text{D}_0 \rightarrow ^7\text{F}_2$  band transitions of the  $\text{Eu}^{3+}$ , respectively. When gold nanoparticles were introduced into the solution containing  $\text{Eu}^{3+}$ , fluorescence emissions at 535 nm, 555 nm, 590 nm are quenched, whereas the  $^5\text{D}_0 \rightarrow ^7\text{F}_2$  emission at 615 nm increased 3 (as shown in Figure 2).

Surface enhanced fluorescence (SEF)<sup>20–26</sup> yields an overall improvement in the fluorescence detection efficiency through modification and control of the local electromagnetic environment of the emitter. Near-field coupling between the emitter and surface modes plays a crucial role in SEF.

In particular, plasmonic surfaces with localized and propagating surface plasmons are efficient SEF substrates. Metallic nanoparticles can influence the fluorescent emission of nearby molecules in several ways: by enhancing the optical intensity incident on the molecule through near field enhancement, by modifying the radiative decay rate of the molecule, or increasing the coupling efficiency of the fluorescence emission to the far field

through nanoparticle scattering. All these processes can be controlled by molecule-nanoparticle separation, nanoparticle size, and geometry.

The geometry and size of the nanoparticles determine the properties of the localized surface plasmons they support. At the plasmon resonance wavelength of a metallic nanoparticle, the light intensity in the near field of the nanoparticle (also known as the fringing field) is enhanced strongly relative to the incident optical wave. The origin of fluorescence enhancement near the nanostructured metal can be understood as arising from two contributions. First, by concentrating the incident light into local electromagnetic "hot spots", nanostructured surfaces can lead to increased absorption of incident light by fluorophores<sup>25–26</sup>. Second, metal nanostructures can alter radiative and nonradiative decay rates of nearby fluorophores, altering both fluorescence lifetime and quantum yield<sup>21–26</sup>.

Our detection of OPA is based on the fact that in the presence of OPA,  $\text{Eu}^{3+}$  ions are released from the gold nanoparticle surface as shown in Scheme 2 and thus a very distinct fluorescence signal change was observed. Fluorescence signal change was observed within a few seconds by a factor of 5 after addition of 4.2  $\mu\text{M}$  of PMP (Figure 2). Since the binding constant of lanthanide ion with OPA is much higher than that of with gold nanoparticle,  $\text{Eu}^{3+}$  was released from the gold nanoparticle surface in the presence of OPA, resulting in fluorescence enhancement in OPA concentration dependent manner (Figure 3). Similar results were obtained for all three OPAs.

To evaluate sensitivity of the NSEF assay, different concentrations of OPA were used to quench the europium fluorescence. As reported before<sup>1–10</sup> that each europium ion binds with 3 OPA (shown in Scheme 2), we have plotted (shown in Figure 4), the NSEF emission intensity change ( $F_0/F$ , where  $F_0$  is the intensity in the absence of OPA and  $F$  is the intensity in the presence of OPA) with one-third concentration of OPA. Our result indicates that NSEF is highly sensitive to the concentration of OPA. The intensity increased linearly with the increase of OPA concentration GLY over the range of 1–25  $\mu\text{M}$  (Figure 4). Therefore, the NSEF probe can provide a quantitative measurement of OPA in aqueous solution.

In conclusion, in this letter we have demonstrated that gold nanoparticle-based NSEF can be used for screening of OPA with high sensitivity (1  $\mu\text{M}$ ) and discussed the role of OPA for fluorescence intensity change in the presence of gold nanoparticle. Linear correlation was found between the emission intensity change and the concentration of the target OPA over the range of 1–25  $\mu\text{M}$ , which indicates that the NSEF probe can provide a quantitative measurement of OPA in aqueous solution. Given the simplicity, quick reaction rate, and sensitivity of this approach, the described methodology could be extended to a high throughput format for OPA agents detection.

## Acknowledgments

Dr. Ray thanks ARO grant # W911NF-06-1-0512, NSF-PREM grant # DMR-0611539, for their generous funding. We also thank reviewers whose valuable suggestion improved the quality of the manuscript.

## References

1. Santiago R, Martínez-Mañez R, Sancenón F, Costero AM, Parra M, Gil S. *Chem. Commun.* 2007:4839.
2. Dale T, Rebek J. J. *Am. Chem. Soc.* 2006; 128:4500. [PubMed: 16594648]
3. Bencic-Nagale S, Sternfeld T, Walt DR. *J. Am. Chem. Soc.* 2006; 128:5041. [PubMed: 16608338]
4. Wang C, Zheng J, Zhao L, Rastogi VK, Shah SS, DeFrank JJ, Leblanc RM. *J. Phys. Chem. B.* 2008; 112:5250. [PubMed: 18373370]

5. Wang J, Zima J, Lawrence NS, Chatrathi MP, Mulchandani A, Collins GE. *Anal. Chem.* 2004; 76:4721. [PubMed: 15307782]
6. Lee CY, Baik S, Zhang J, Masel RI, Strano MS. *J. Phys. Chem. B.* 2006; 110:11055. [PubMed: 16771365]
7. Newman JDS, Roberts JM, Blanchard GJ. *Anal. Chem.* 2007; 79:3448. [PubMed: 17378539]
8. Wang C, Li C, Ji X, Orbulescu J, Xu J, Leblanc RM. *Langmuir.* 2006; 22:2200. [PubMed: 16489807]
9. Halamek J, Pribyl J, Makower A, Skladal P, Scheller FW. *Anal. Bioanal. Chem.* 2005; 382:1904. [PubMed: 15906004]
10. Seferos SD, Giljohann DA, Hill D, Progodich AE, Morkin CA. *J. Am. Chem. Soc.* 2007; 129:15477. [PubMed: 18034495]
11. Skewis LR, Reinhard BM BM. *Nano Lett.* 2008; 8:214. [PubMed: 18052230]
12. Alvarez-Puebla RA, Nazri G-A, Aroca RF. *J. Mater. Chem.* 2006; 16:2921.
13. Ray PC. *Angew. Chem. Int. Ed.* 2006; 45:1151.
14. Darbha GK, Singh AK, Rai US, Yu E, Yu H, Ray PC. *J. Am. Chem. Soc.* 2008 in press.
15. Bonham AJ, Braun G, Pavel I, Moskovits M, Reich NO. *J. Am. Chem. Soc.* 2007; 129:14572. [PubMed: 17985912]
16. Huang X, El-Sayed IH, Qian W, El-Sayed MA. *J. Am. Chem. Soc.* 2006; 128:2115. [PubMed: 16464114]
17. Darbha GK, Ray A, Ray PC. *ACS Nano.* 2007; 1:208. [PubMed: 19206651]
18. Tiwari VS, Oleg T, Darbha GK, Hardy W, Singh JP, Ray PC. *Chemical Physics Letters.* 2007; 446:77.
19. Ray PC, Fortner A, Griffin J, Kim C, Singh JP, Yu H. *Chem. Phys. Lett.* 2005; 414:259.
20. Zhang Y, Aslan K, Previte MJR, Geddes CD. *Chem. Phys. Lett.* 2006; 432:528. [PubMed: 18071576]
21. Liu GL, Rosa-Bauza YT, Salisbury CM, Craik C, Ellman JA, Chen FF, Lee LP. *J. Nanosci. Nanotech.* 2007; 7:2323.
22. Zhang J, Malicka J, Gryczynski I, Lakowicz LR. *J. Phys. Chem. B.* 2005; 109:7643. [PubMed: 16851886]
23. Xie F, Baker MS, Goldys EM. *J. Phys. Chem. B.* 2006; 110:23085. [PubMed: 17107148]
24. Aslan K, Huang J, Wilson GM, Geddes CD. *J. Am. Chem. Soc.* 2006; 128:4206. [PubMed: 16568977]
25. Bek A, Jansen R, Ringler M, Mayilo S, Klar TA, Feldmann J. *Nano Lett.* 2008; 8:485. [PubMed: 18173294]
26. Jain PK, Huang X, El-Sayed IH, El-Sayed MA. *Acc. Chem. Res.* 2008 ASAP Article.
27. Ray PC, Fortner A, Darbha GK. *J. Phys. Chem. B.* 2006; 110:20745. [PubMed: 17048879]
28. Ray PC, Darbha GK, Ray A, Hardy W, Walker J. *Nanotechnology.* 2007; 18:375504.
29. Darbha GK, Rai US, Singh AK, Ray PC. *Chem. Eur. J.* 2008; 14, 3896.
30. Ryan BC, Kwong GA, Radu CG, Witte ON, Heath JR. *J. Am. Chem. Soc.* 2007; 129:129, 1959.
31. Nam JM, Thaxton CS, Mirkin CA. *Science.* 2003; 301:1884. [PubMed: 14512622]
32. Carsten S, Snnichsen A, Reinhard BM, Liphardt J, Alivisatos PA. *Nature Biotechnology.* 2005; 23:741.
33. Maxwell DJ, Taylor JR, Nie S S. *J. Am. Chem. Soc.* 2002; 124:9602.
34. Lewis DJ, Day TM, MacPherson JV, Pikramenou Z. *Chem. Comm.* 2006:1433. [PubMed: 16550291]
35. Itty IB, Thomas YK, George K. *J. Am. Chem. Soc.* 2006; 128:1907. [PubMed: 16464092]

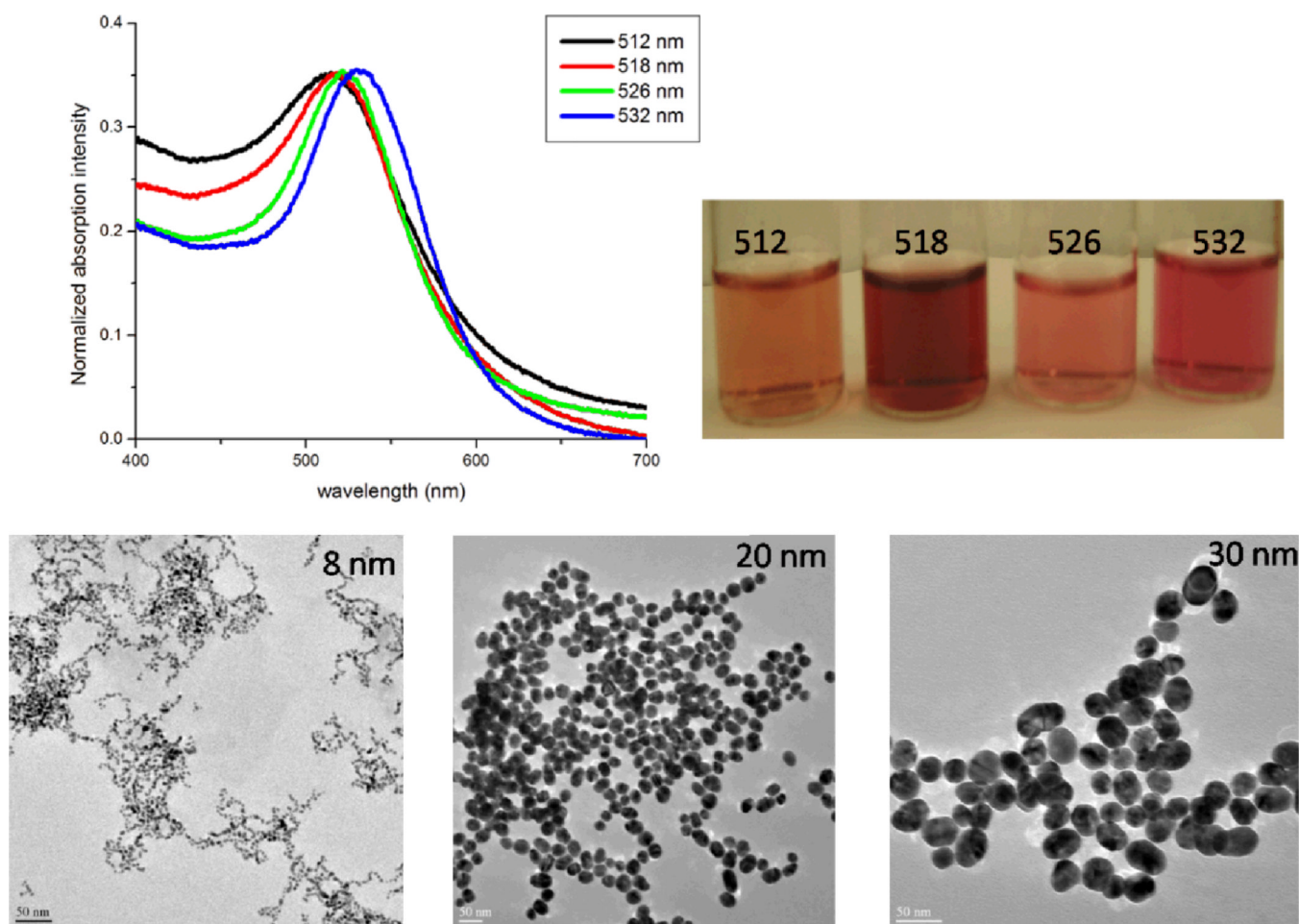


**Figure 1.** Absorption spectra, photograph and TEM of gold nanospheres of different sizes

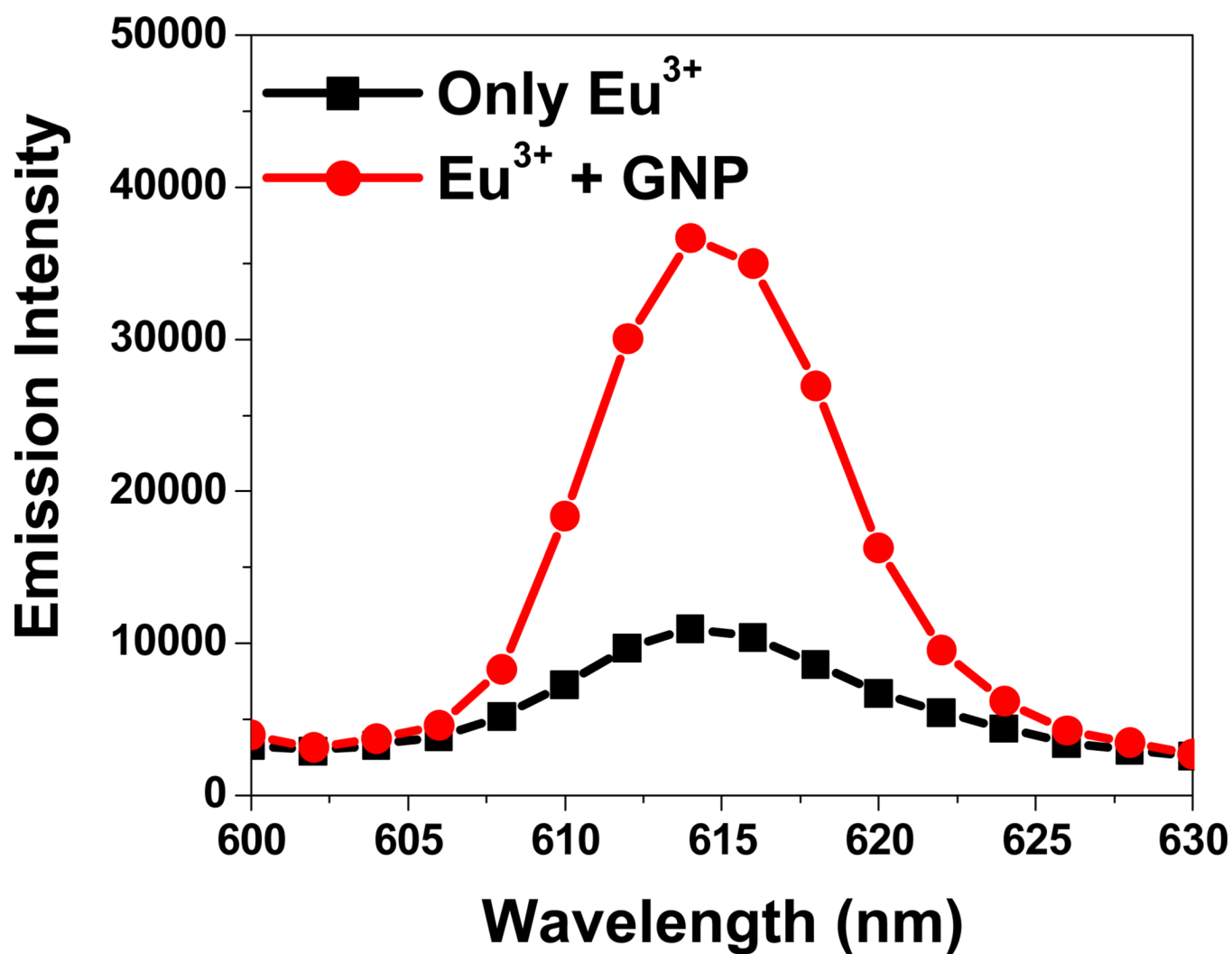


**Figure 2.**  
Enhancement of Emission intensity in the presence of gold nanoparticle

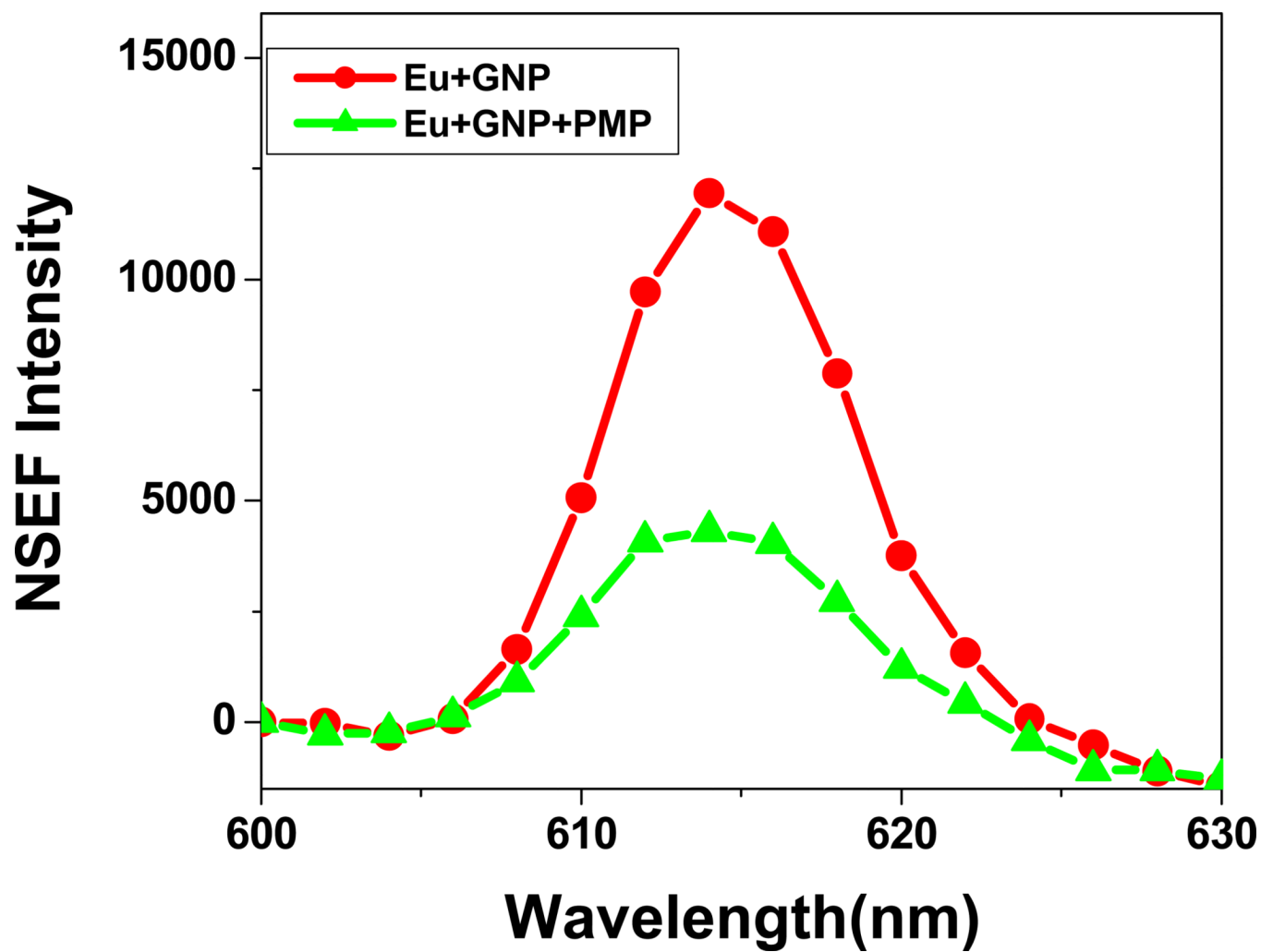


**Figure 3.**  
NSEF intensity before and after addition of glyphosate

NSFE Intensity Ratio

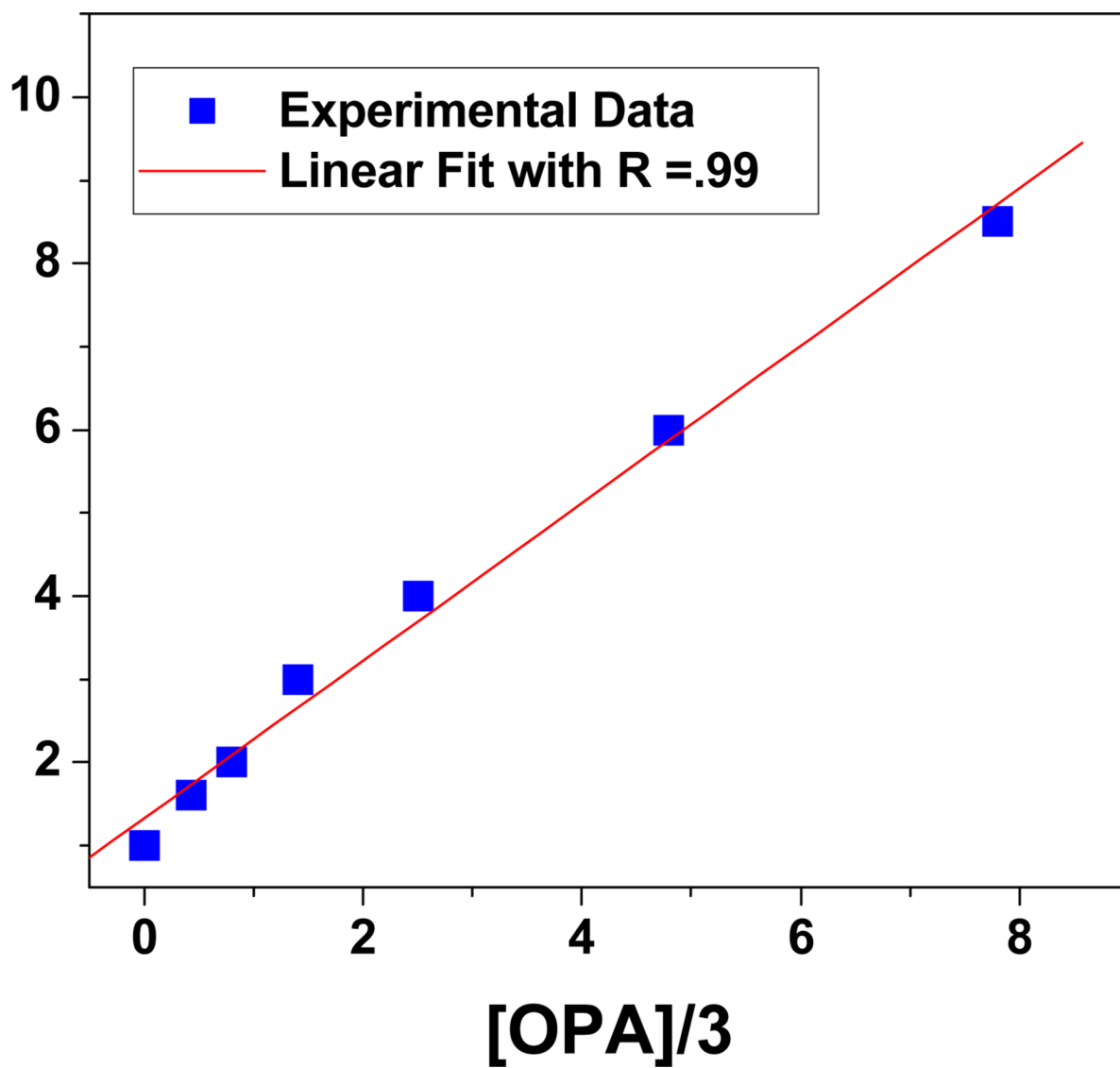
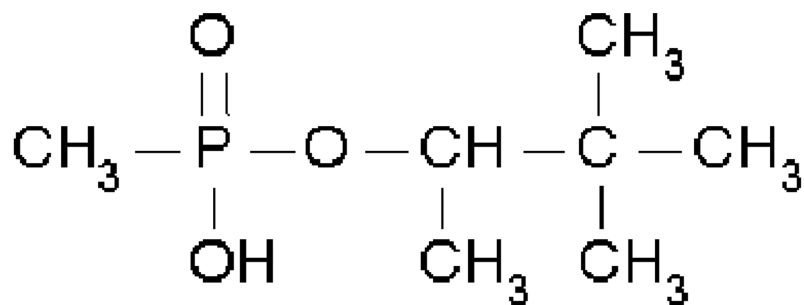
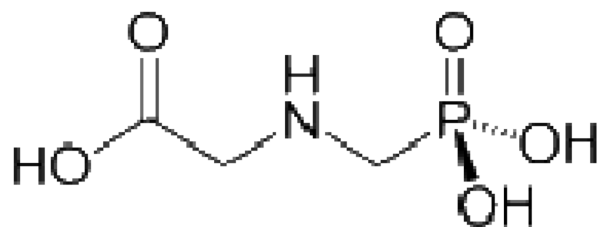


**Figure 4.**  
Linear plot of NSEF intensity vs. one third concentration of glyphosate

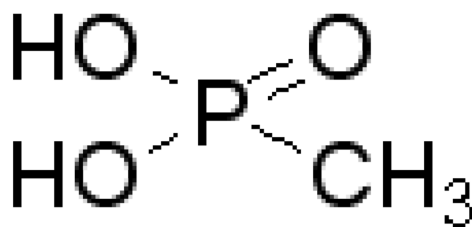




### PINACOLYL METHYLPHOSPHATE (PMP)



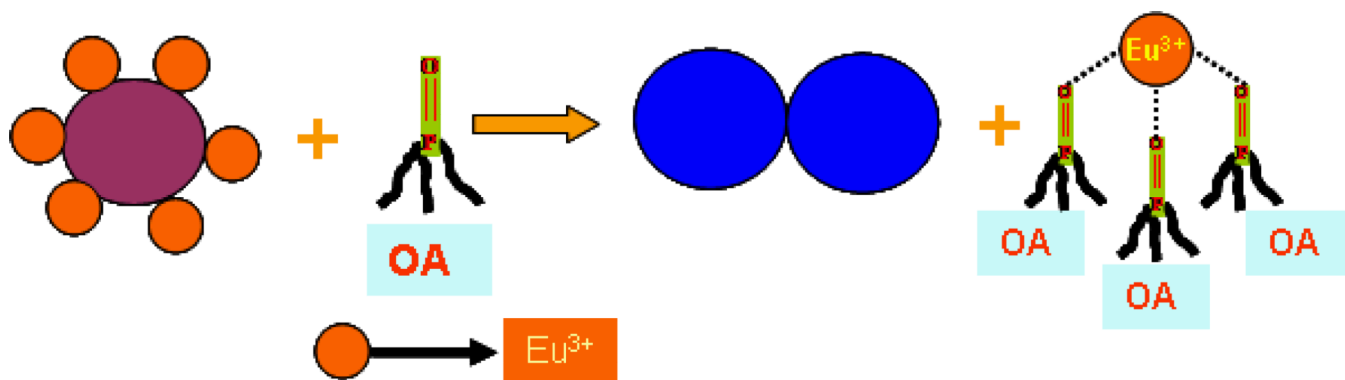
### GLYPHOSATE (GLY)



### METHYLPHOSPHONIC ACID (MPA)

**Scheme 1.**

Scheme of organophosphorus agents used in this manuscript.



**Scheme 2.**  
Schematic representation of NSEF assay for OPA detection